SPACE-TIME MULTIPATCH DISCONTINUOUS GALERKIN ISOGEOMETRIC ANALYSIS FOR PARABOLIC EVOLUTION PROBLEMS[*]

STEPHEN EDWARD MOORE[†]

Abstract. We present and analyze a stable space-time multipatch discontinuous Galerkin iso-geometric analysis (dGIGA) scheme for the numerical solution of parabolic evolution equations in deforming space-time computational domains. Following [S. E. Moore, *Nonstandard Discretization Strategies in Isogeometric Analysis for Partial Differential Equations,* Ph. D. thesis, 2017; S. E. Moore, *Calcolo,* 55 (2018), 18], we use a time-upwind test function and apply multipatch dGIGA methodology for discretizing the evolution problem both in space and in time. This yields a discrete bilinear form which is elliptic on the IGA space with respect to a space-time dG norm. This prop-erty together with a corresponding boundedness property and consistency and approximation results for the IGA spaces yields an *a priori discretization* error estimate with respect to the space-time dG norm. The theoretical results are confirmed by several numerical experiments with low- and high-order IGA spaces.

Key words. parabolic initial-boundary value problems, space-time, discontinuous Galerkin, isoeometric analysis, multipatch, deforming computational domains, a priori error estimates

AMS subject classifications. 65N12, 65N15, 65N30

DOI. 10.1137/17M1140285

1. Introduction. Several discretization methods exists for solving parabolic evolution problems. The standard discretization methods in time and space are based on time-stepping methods combined with some spatial discretization techniques like finite element methods, finite difference methods, finite volume methods, etc. The two main time-stepping methods are horizontal and vertical methods of lines. The vertical method of lines discretizes first in space and then in time, whereas in the hor-izontal method of lines, also known as Rothe's method, the discretization starts with respect to the time variable; see, e.g., [20, 17, 32]. However, due to the separation of space and time discretizations, the development of efficient and fully adaptive schemes becomes complicated. This also affects negatively the parallelization of solvers due to the curse of sequentiality.

Another approach to discretization of parabolic evolution problems is the space-time methods. The space-time schemes allow for discretization in space and time simultaneously; see, e.g., [13, 34]. Space-time and space-time discontinuous Galerkin (dG) discretization and their applications to several partial differential equations in-cluding their adaptivity and the treatment of changing spatial domains in time have been addressed; for example, see [31, 6, 25] and [26] and all references therein. Space-time dG has been applied to incompressible and compressible Navier–Stokes equa-tions; see, e.g., [27, 16].

Many approximation schemes have been developed for space-time formulation of parabolic evolution problems. Particularly, p and hp in time versions of the hp-finite element method to parabolic problems have been investigated in [2] and [3], respectively. This was followed by hp dG time-stepping combined with FEM in space;

[†]Department of Mathematics, University of Cape Coast, Cape Coast, Ghana (stephen.moore@ucc.edu.gh).

see [28]. Also, space-time wavelet methods for parabolic evolution problems have been analyzed in [29, 8]. Error bounds for reduced basis approximation (see, e.g., [33]) and uniform stability of an abstract Petrov–Galerkin discretization of boundedly invertible operators for space-time discretizations to linear parabolic problems have been studied in [1]. Space-time streamline diffusion methods which use special time-upwind test functions have also been applied to Navier–Stokes and other engineering problems; see, e.g., [11, 14].

Another numerical scheme that has been introduced in recent times is isogeometric analysis (IGA). IGA was introduced by Hughes, Cottrel, and Bazilevs in 2005 (see, e.g., [12]) and uses the same basis functions for both representing the approximate solution and the geometry description. In [5], the authors introduced approximation, stability, and error estimates for h-refined IGA meshes of spatial computational domains; see also [30]. The tools involved in the analysis and experimentation of the scheme are computational domain Q, a geometrical mapping Φ, and a parameter domain $\widehat{Q}$. The computational domain, also called patch, can involve one or several domains. In most industrial applications, the computational domains involve several domains or patches. Several assembling strategies involving multiple patches have been presented in IGA, including mortar methods [7] and dG methods [21].

In [21], the dGIGA was presented where the approximation estimates are valid for each patch including nonmatching meshes. Using these approximation results for B-splines or NURBS together with the ellipticity of the discrete bilinear form $a_h(\cdot, \cdot)$ with respect to a discrete norm $\| \cdot \|_h$ with boundedness and consistency results, asymptotically optimal discretization error estimates in the discrete dGIGA norm $\| \cdot \|_h$ were obtained.

The aim of this paper is to present a new stable space-time multipatch dGIGA scheme for the numerical approximation of parabolic initial-boundary value problems. In this approach, the time variable t is considered as just another variable x_{d+1} if $x_1, \ldots, x_d$ are the spatial variables. In this sense, the time derivative acts as a strong convection term in the direction x_{d+1}; see, e.g., [25, 31, 4]. The current article is motivated by an earlier article [23], where a single-patch moving and a non-moving spatial computational domain were considered. The space-time cylinder Q was represented by one smooth, uniformly regular B-spline or NURBS map Φ of the parameter domain $\widehat{Q} = (0,1)^{d+1}, d \in \{1, 2, 3\}$. However, in this paper, we consider multipatch coupling in both space and time where we penalize the interfaces via penalty parameters. By using a time-upwind test function, we derive a discrete bilinear form $a_h(\cdot, \cdot) : V_{0h} \times V_{0h} \to \mathbb{R}$ which is elliptic on the space-time dGIGA space V_{0h} with respect to a discrete space-time norm $\| \cdot \|_h$. The analysis of the space-time dGIGA scheme follows the monograph of Di Pietro and Ern [10] and requires three main ingredients, namely, discrete coercivity, consistency, and boundedness of the discrete bilinear form.

The rest of the paper is organized as follows. In section 2, we introduce the model problem and variational formulation. We also present tools necessary for the IGA. In section 3, we will present the derivation of the stable space-time multipatch dGIGA. Section 4 will deal with the approximation results and, finally, the a priori error estimate. We will present numerical results to confirm the theory in section 5.

2. Model problem and method. Let us first introduce the Sobolev spaces $H^{s_x, s_t}(Q) = \{u \in L_2(Q) : \partial_x^\alpha u \in L_2(Q) \text{ for all } \alpha \text{ with } 0 \leq |\alpha| \leq s_x, \partial_t^i u \in L_2(Q), i = 0, \ldots, s_t\}$ of functions defined in the space-time cylinder Q, where $L_2(Q)$ denotes the space of square-integrable functions, $\alpha = (\alpha_1, \ldots, \alpha_d)$ is a multi-index with non-

negative integers $\alpha_1, \ldots, \alpha_d$, $|\alpha| = \alpha_1 + \cdots + \alpha_d$, $\partial_x^\alpha u := \partial^{|\alpha|} u / \partial x^\alpha = \partial^{|\alpha|} u / \partial x_1^{\alpha_1} \cdots \partial x_d^{\alpha_d}$, and $\partial_t^i u := \partial^i u / \partial t^i$; see, e.g., [18].

2.1. Model problem. We consider a linear parabolic initial-boundary value problem: find $u : \overline{Q} \to \mathbb{R}$ such that

$$(2.1) \qquad \partial_t u - \Delta u = f \quad \text{in} \quad Q, \quad u = 0 \quad \text{on} \quad \Sigma \cup \Sigma_0,$$

as the model problem posed in the space-time cylinder $\overline{Q} = \overline{\Omega(t)} \times [0, T]$, where Δ is the Laplace operator, ∂_t denotes the partial time derivative, $f \in L_2(Q)$ is a given source function, T is the final time, and $\Omega(t) \subset \mathbb{R}^d$, $d \in \{1, 2, 3\}$, denotes the spatial computational domain with the boundary $\partial \Omega(t)$. We consider that the computational domain Q is bounded and Lipschitz with $\Sigma := \partial \Omega(t) \times (0, T)$ and $\Sigma_0 = \Omega(0) \times \{0\}$.

The standard weak space-time variational formulation of (2.1) reads as follows: find $u \in H_{0,\underline{0}}^{1,0}(Q)$ such that

$$(2.2) \qquad a(u, v) = \ell(v) \quad \forall v \in H_{0,\overline{0}}^{1,1}(Q),$$

with the bilinear and linear forms given by

$$(2.3) \qquad a(u, v) = - \int_Q u \partial_t v \, dx dt + \int_Q \nabla_x u \cdot \nabla_x v \, dx dt \quad \text{and} \quad \ell(v) = \int_Q f v \, dx dt,$$

where the trial and test functions are defined by $H_{0,\underline{0}}^{1,0}(Q) = \{u \in L_2(Q) : \nabla_x u \in [L_2(Q)]^d, u = 0 \text{ on } \Sigma, \text{ and } u = 0 \text{ on } \Sigma_0\}$ and $H_{0,\overline{0}}^{1,1}(Q) = \{u \in L_2(Q) : \nabla_x u \in [L_2(Q)]^d, \partial_t u \in L_2(Q), u = 0 \text{ on } \Sigma, \text{ and } u = 0 \text{ on } \Sigma_T\}$. We denote $\Sigma_T := \Omega(T) \times \{T\}$, and $\nabla_x u = (\partial u / \partial x_1, \ldots, \partial u / \partial x_d)^\top$ denotes the gradient with respect to the spatial variables. The variational problem (2.2), including more general parabolic initial-boundary value problems, and other boundary conditions and more general elliptic parts, and nonlinear versions are known to have a unique weak solution; see, e.g., [18, 35, 32].

2.2. B-spline and NURBS isogeometric analysis. B-spline and NURBS based Galerkin methods have been studied and presented in the monograph [9]. Here, we present briefly some information on the construction of the B-spline. Let us consider an interval $[0, 1]$, a vector $\Xi = \{0 = \xi_1, \ldots, \xi_{n+p+1} = 1\}$ with $p \geq 1$, and n the number of basis functions. A *knot vector* is a nondecreasing sequence of real numbers in the unit interval also called parameter domain $[0, 1]$. The knot vector Ξ defines the univariate B-spline basis functions via the Cox–de Boor recursion formula

$$\widehat{B}_{i,0}(\xi) = \begin{cases} 1 & \text{if} \quad \xi_i \leq \xi < \xi_{i+1}, \\ 0 & \text{else}, \end{cases}$$

$$(2.4) \qquad \widehat{B}_{i,p}(\xi) = \frac{\xi - \xi_i}{\xi_{i+p} - \xi_i} \widehat{B}_{i,p-1}(\xi) + \frac{\xi_{i+p+1} - \xi}{\xi_{i+p+1} - \xi_{i+1}} \widehat{B}_{i+1,p-1}(\xi),$$

where a division by zero is defined to be zero. We note that a basis function of degree p is $(p-m)$ times continuously differentiable across a knot value with the multiplicity m. If all internal knots have the multiplicity $m = 1$, then B-splines of degree p are globally C^{p-1}-continuous.

In general for $(d+1)$-dimensional problems, the B-spline basis functions are tensor products of the univariate B-spline basis functions. Let $\Xi_\alpha = \{\xi_{1,\alpha}, \ldots, \xi_{n_\alpha + p_\alpha + 1, \alpha}\}$ be the knot vectors for every direction $\alpha = 1, \ldots, d + 1$. The tensor product B-spline basis functions are defined by

$$(2.5) \qquad \widehat{B}_{\mathbf{i}, \mathbf{p}}(\xi) := \prod_{\alpha=1}^{d+1} \widehat{B}_{i_\alpha, p_\alpha}(\xi_\alpha),$$

where $\xi = (\xi_1, \ldots, \xi_{d+1}) \in \widehat{Q} = (0,1)^{d+1}$. The univariate and multivariate B-spline basis functions are defined in the parametric domain by means of the corresponding B-spline basis functions $\{\widehat{B}_{\mathbf{i},\mathbf{p}}\}_{\mathbf{i}\in\overline{\mathcal{I}}}$. The distinct values of the knot vectors Ξ provide a partition of $(0,1)^{d+1}$ creating a mesh $\widehat{\mathcal{K}}_h$ in the parameter domain where $\widehat{K}$ is a mesh element; see, e.g., Figure 1.
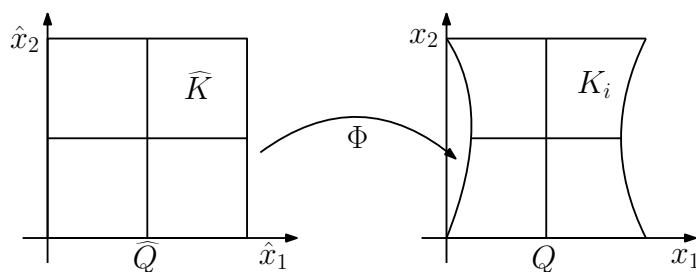

FIG. 1. *The mesh underlying the physical domain* ($\mathcal{K}_h$) *and parametric domain* ($\widehat{\mathcal{K}}_h$).

The computational domain is described by means of a geometrical mapping $\mathbf{\Phi}$ such that $Q = \mathbf{\Phi}(\widehat{Q})$ and

$$(2.6) \qquad \mathbf{\Phi}(\xi) := \sum_{\mathbf{i}\in\overline{\mathcal{I}}} C_{\mathbf{i}}\widehat{B}_{\mathbf{i},\mathbf{p}}(\xi),$$

where $C_{\mathbf{i}}$ are the control points. We define the basis functions in the computational domain by means of the geometrical mapping as $B_{\mathbf{i},\mathbf{p}} := \widehat{B}_{\mathbf{i},\mathbf{p}} \circ \mathbf{\Phi}^{-1}$ and the discrete function space by

$$(2.7) \qquad \mathbb{V}_h = \mathrm{span}\{B_{\mathbf{i},\mathbf{p}} : \mathbf{i} \in \overline{\mathcal{I}}\};$$

for the sake of the current work, we assume $\mathbb{V}_h \subset H^s(Q), s \geq 2$, i.e., continuously differentiable (C^1) basis functions on each patch. In many practical applications,
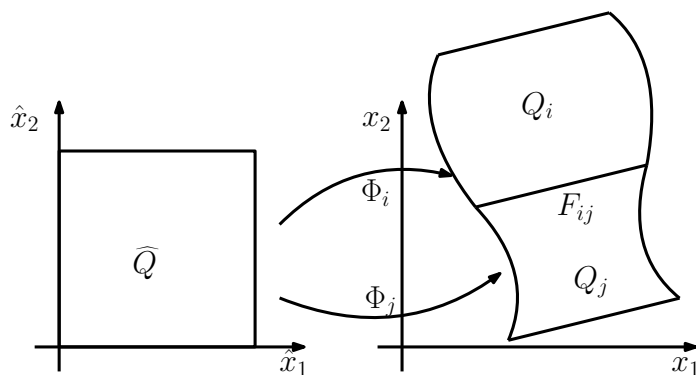

FIG. 2. *A representation of the multipatch space-time mapping from the parameter domain to the physical domain.*

the computational domain Q is decomposed into N nonoverlapping domain Q_i called subdomains or patches denoted as $\mathcal{T}_h := \{Q_i\}_{i=1}^N$ such that $\overline{Q} = \bigcup_{i=1}^N \overline{Q}_i$ and $Q_i \cap Q_j = \emptyset$ for $i \neq j$. Each patch is the image of an associated geometrical mapping $\mathbf{\Phi}_i$ such that $\mathbf{\Phi}_i(\widehat{Q}) = Q_i, i = 1, \ldots, N$; see Figure 2.

Let $F_{ij} = \partial Q_i \cap \partial Q_j, i \neq j$, denote the interior facets of two patches. The collection of all such interior facets is denoted by $\mathcal{F}_I$, and the collection of all Dirichlet facets $F_i = \partial Q_i \cap \partial Q$ is also denoted by $\mathcal{F}_D$. The set of facets F_i on Σ_T is denoted by $\mathcal{F}_T$ and the facet F_i on Σ_0 by $\mathcal{F}_0$. Furthermore, the collection of all internal and Dirichlet facets is denoted by $\mathcal{F} := \mathcal{F}_I \cup \mathcal{F}_D \cup \mathcal{F}_0 \cup \mathcal{F}_T$.

Also, we assume that for each patch $Q_i, i = 1, \ldots, N$, the underlying mesh $\mathcal{K}_{h,i}$ is quasi-uniform, i.e.,

$$(2.8) \qquad h_K \leq h_i \leq C_q h_K \quad \forall \quad K \in \mathcal{K}_{h,i}, \quad i = 1, \ldots, N,$$

where $C_q \geq 1$ and $h_i = \max\{h_K, K \in \mathcal{K}_{h,i}\}$ is the mesh size of Q_i and h_K is the diameter of the mesh element K. Finally, the multipatch discrete function space is given as

$$(2.9) \qquad V_h = \{v \in L^2(Q) : v|_{Q_i} \in \mathbb{V}_{h,i} \; \forall i = 1, \ldots, N\}.$$

3. Stable space-time discontinuous Galerkin isogeometric analysis. For a nonoverlapping decomposition of the space-time computational domain Q into N patches, we assign nonnegative integers s_i to each patch Q_i and collect them in the vector $\mathbf{s} = \{s_1, \ldots, s_N\}$. Let us now define the broken Sobolev space

$$(3.1) \qquad H^{\mathbf{s}}(Q, \mathcal{T}_h) := \{v \in L_2(Q) : v|_{Q_i} \in H^{s_i}(Q_i) \; \forall i = 1, \ldots, N\},$$

and equip it with a broken Sobolev norm and seminorm

$$(3.2)$$

$$\|v\|_{H^{\mathbf{s}}(Q,\mathcal{T}_h)} := \left(\sum_{i=1}^{N} \|v\|^2_{H^{s_i}(Q_i)} \right)^{1/2} \quad \text{and} \quad |v|_{H^{\mathbf{s}}(Q,\mathcal{T}_h)} := \left(\sum_{i=1}^{N} |v|^2_{H^{s_i}(Q_i)} \right)^{1/2},$$

respectively.

Next, we define the function spaces

$$(3.3) \qquad V_{0h} := V_h \cap H^{1,1}_{0,\underline{0}}(Q) \quad \text{and} \quad V_{0h,*} := H^{1,0}_0(Q) \cap H^2(Q) + V_{0h}.$$
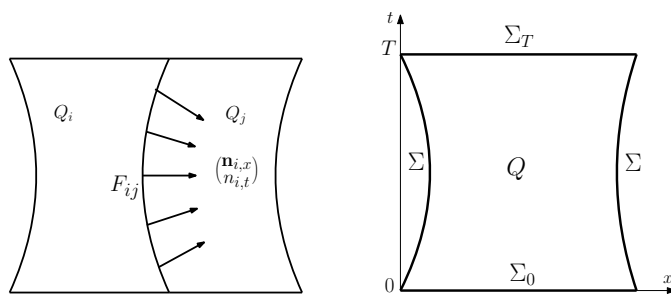

FIG. 3. *A representation of the interface F_{ij} of two neighboring patches Q_i and Q_j and its associated normal vector $\mathbf{n}_i = (\mathbf{n}_{i,x}, n_{i,t})$ on the left. The underlying physical mesh (blue) for the multipatch on the right.*

DEFINITION 3.1. *Let $F_{ij} \in \mathcal{F}_I$ be an interior facet with the outer unit normal vector $\mathbf{n}_i = (\mathbf{n}_{i,x}, n_{i,t})^\top \in \mathbb{R}^{d+1}$ with respect to $Q_i \subset \mathbb{R}^{d+1}$ with $d \in \{1, 2, 3\}$. For a given, sufficiently smooth function v with values in $\mathbb{R}$ or $\mathbb{R}^{d+1}$, we will denote the*

restriction of the function v to Q_i and Q_j by v_i and v_j, respectively. We define the jumps across the facets by

$$[\![v]\!] := \begin{cases} v_i^\top \mathbf{n}_i + v_j^\top \mathbf{n}_j & on \quad F_{ij} \in \mathcal{F}_I, \\ v_i^\top \mathbf{n}_i & on \quad F_i \in \mathcal{F} \setminus \mathcal{F}_I. \end{cases}$$

For v having values in $\mathbb{R}$ or $\mathbb{R}^d$, the jump in space direction is given by

$$[\![v]\!]_x := \begin{cases} v_i^\top \mathbf{n}_{i,x} + v_j^\top \mathbf{n}_{j,x} & on \quad F_{ij} \in \mathcal{F}_I, \\ v_i^\top \mathbf{n}_{i,x} & on \quad F_i \in \mathcal{F} \setminus \mathcal{F}_I, \end{cases}$$

whereas the jump in time direction is defined by

$$[\![v]\!]_t := \begin{cases} v_i n_{i,t} + v_j n_{j,t} & on \quad F_{ij} \in \mathcal{F}_I, \\ v_i n_{i,t} & on \quad F_i \in \mathcal{F} \setminus \mathcal{F}_I. \end{cases}$$

The average of function v is nothing but

$$\{v\} := \begin{cases} \dfrac{1}{2}(v_i + v_j) & on \quad F_{ij} \in \mathcal{F}_I, \\ v_i & on \quad F_i \in \mathcal{F} \setminus \mathcal{F}_I. \end{cases}$$

For the interior facets $F_{ij} \in \mathcal{F}_I$, the upwind in time direction is given by

$$(3.4) \qquad \{v\}^{up} := \begin{cases} v_i & for \quad n_{i,t} \geq 0, \\ v_j & for \quad n_{i,t} < 0, \end{cases}$$

whereas the downwind in time direction is given by

$$(3.5) \qquad \{v\}^{down} := \begin{cases} v_j & for \quad n_{i,t} \geq 0, \\ v_i & for \quad n_{i,t} < 0. \end{cases}$$

The derivation of the variational scheme requires some formulas stated in the next lemma.

LEMMA 3.2. *Let $F_{ij} \in \mathcal{F}_I$ be an interface, and let u and v be sufficiently smooth functions. Then the following formulas hold:*

$$(3.6) \qquad\qquad [\![uv]\!]_x = \{u\}[\![v]\!]_x + \{v\}[\![u]\!]_x,$$

$$(3.7) \qquad\qquad [\![uv]\!]_t = \{u\}^{up}[\![v]\!]_t + \{v\}^{down}[\![u]\!]_t.$$

Proof. See, e.g., [24, Lemma 5.17]. □

We will begin with the derivation of the space-time multipatch dGIGA scheme as follows. We multiply the model problem (2.1) by a time-upwind test function $v_h + \theta h \partial_t v_h$ with an arbitrary $v_h \in V_{0h}$ with a positive constant θ and sum over each patch

$$\sum_{i=1}^N \int_{Q_i} f(v_h + \theta_i h_i \partial_t v_h) \, dx dt$$

$$(3.8) \qquad = \sum_{i=1}^N \int_{Q_i} \left(\partial_t u(v_h + \theta_i h_i \partial_t v_h) - \Delta u(v_h + \theta_i h_i \partial_t v_h) \right) dx dt.$$

Concerning the Laplacian term Δu, we sum over each patch and apply an integration by parts with respect to the spatial direction leading to

$$-\sum_{i=1}^{N} \int_{Q_i} \Delta u(v_h + \theta_i h_i \partial_t v_h)\, dxdt = \sum_{i=1}^{N} \int_{Q_i} \left(\nabla_x u \cdot \nabla_x v_h + \theta_i h_i \nabla_x u \cdot \nabla_x \partial_t v_h \right) dxdt$$

$$(3.9) \qquad\qquad\qquad\qquad\qquad\qquad - \sum_{i=1}^{N} \int_{\partial Q_i} \mathbf{n}_{i,x} \cdot \nabla_x u(v_h + \theta_i h_i \partial_t v_h)\, ds.$$

Integrating by parts the first term with respect to the time yields

$$= \sum_{i=1}^{N} \int_{Q_i} \left(\nabla_x u \cdot \nabla_x v_h - \theta_i h_i \partial_t \nabla_x u \cdot \nabla_x v_h \right) dxdt$$

$$(3.10) \quad + \theta_i h_i \sum_{i=1}^{N} \int_{\partial Q_i} n_{i,t} \nabla_x u \cdot \nabla_x v_h\, ds - \sum_{i=1}^{N} \int_{\partial Q_i} \left(\mathbf{n}_{i,x} \cdot \nabla_x u(v_h + \theta_i h_i \partial_t v_h) \right) ds.$$

By considering the boundary terms in (3.10), we rewrite the sum over the boundary integrals as

$$\theta_i h_i \sum_{i=1}^{N} \int_{\partial Q_i} (n_{i,t} \nabla_x u \cdot \nabla_x v_h)\, ds = \theta_i h_i \sum_{F_{ij} \in \mathcal{F}_I} \int_{F_{ij}} [\![\nabla_x u \cdot \nabla_x v_h]\!]_t\, ds$$

$$(3.11) \qquad\qquad\qquad\qquad\qquad + \theta_i h_i \sum_{F_i \in \mathcal{F}_0 \cup \mathcal{F}_T \cup \mathcal{F}_D} \int_{F_i} n_{i,t} \nabla_x u \cdot \nabla_x v_h\, ds$$

and

$$\sum_{i=1}^{N} \int_{\partial Q_i} \left(\mathbf{n}_{i,x} \cdot \nabla_x u(v_h + \theta_i h_i \partial_t v_h) \right) ds$$

$$= \sum_{F_{ij} \in \mathcal{F}_I} \int_{F_{ij}} [\![\nabla_x u v_h]\!]_x\, ds + \theta_i h_i \sum_{F_{ij} \in \mathcal{F}_I} \int_{F_{ij}} [\![\nabla_x u \partial_t v_h]\!]_x\, ds$$

$$(3.12) \qquad + \sum_{F_i \in \mathcal{F}_0 \cup \mathcal{F}_T \cup \mathcal{F}_D} \int_{F_i} \mathbf{n}_{i,x} \cdot \nabla_x u(v_h + \theta_i h_i \partial_t v_h)\, ds.$$

Since $v_h = 0$ on the facets $F_i \in \mathcal{F}_0$, the term (3.11) yields

$$\theta_i h_i \sum_{i=1}^{N} \int_{\partial Q_i} (n_{i,t} \nabla_x u \cdot \nabla_x v_h)\, ds = \theta_i h_i \sum_{F_{ij} \in \mathcal{F}_I} \int_{F_{ij}} [\![\nabla_x u \cdot \nabla_x v_h]\!]_t\, ds$$

$$(3.13) \qquad\qquad\qquad\qquad\qquad + \theta_i h_i \sum_{F_i \in \mathcal{F}_T \cup \mathcal{F}_D} \int_{F_i} n_{i,t} \nabla_x u \cdot \nabla_x v_h\, ds.$$

The normal vector in the space direction $\mathbf{n}_{i,x}$ is zero for $F_i \in \mathcal{F}_0$ and $F_i \in \mathcal{F}_T$; thus (3.12) can be rewritten as

$$\sum_{i=1}^{N} \int_{\partial Q_i} \left(\mathbf{n}_{i,x} \cdot \nabla_x u(v_h + \theta_i h_i \partial_t v_h) \right) ds$$

$$= \sum_{F_{ij} \in \mathcal{F}_I} \int_{F_{ij}} [\![\nabla_x u v_h]\!]_x\, ds + \theta_i h_i \sum_{F_{ij} \in \mathcal{F}_I} \int_{F_{ij}} [\![\nabla_x u \partial_t v_h]\!]_x\, ds$$

$$(3.14) \qquad + \theta_i h_i \sum_{F_i \in \mathcal{F}_D} \int_{F_i} \mathbf{n}_{i,x} \cdot \nabla_x u \partial_t v_h\, ds.$$

Substituting (3.13) and (3.14) into (3.10) and rearranging the terms yields

$$
-\sum_{i=1}^{N}\int_{Q_i}\Delta u(v_h+\theta_i h_i\partial_t v_h)\,dxdt
$$

$$
=\sum_{i=1}^{N}\int_{Q_i}\left(\nabla_x u\cdot\nabla_x v_h-\theta_i h_i\partial_t\nabla_x u\cdot\nabla_x v_h\right)dxdt
$$

$$
+\theta_i h_i\sum_{F_i\in\mathcal{F}_T}\int_{F_i}n_{i,t}\nabla_x u\cdot\nabla_x v_h\,ds+\theta_i h_i\sum_{F_{ij}\in\mathcal{F}_I}\int_{F_{ij}}[\![\nabla_x u\cdot\nabla_x v_h]\!]_t\,ds
$$

$$
-\sum_{F_{ij}\in\mathcal{F}_I}\int_{F_{ij}}\left([\![\nabla_x u v_h]\!]_x+\theta_i h_i[\![\nabla_x u\partial_t v_h]\!]_x\right)ds
$$

$$
+\theta_i h_i\sum_{F_i\in\mathcal{F}_D}\int_{F_i}\left(n_{i,t}\nabla_x u\cdot\nabla_x v_h-\mathbf{n}_{i,x}\cdot\nabla_x u\partial_t v_h\right)ds.
$$

Now, by using Lemma 3.2, which also holds for vector functions, we can rewrite the terms on the interior facets F_{ij} to obtain

$$
=\sum_{i=1}^{N}\int_{Q_i}\left(\nabla_x u\cdot\nabla_x v_h-\theta_i h_i\partial_t\nabla_x u\cdot\nabla_x v_h\right)dxdt+\theta_i h_i\sum_{F_i\in\mathcal{F}_T}\int_{F_i}\nabla_x u\cdot\nabla_x v_h\,ds
$$

$$
+\theta_i h_i\sum_{F_{ij}\in\mathcal{F}_I}\int_{F_{ij}}\left(\{\nabla_x u\}^{up}[\![\nabla_x v_h]\!]_t+\{\nabla_x v_h\}^{down}[\![\nabla_x u]\!]_t\right)ds
$$

$$
-\sum_{F_{ij}\in\mathcal{F}_I}\int_{F_{ij}}\left(\{\nabla_x u\}[\![v_h]\!]_x+[\![\nabla_x u]\!]_x\{v_h\}\right)ds
$$

$$
-\theta_i h_i\sum_{F_{ij}\in\mathcal{F}_I}\int_{F_{ij}}\left(\{\nabla_x u\}[\![\partial_t v_h]\!]_x+[\![\nabla_x u]\!]_x\{\partial_t v_h\}\right)ds
$$

$$
+\theta_i h_i\sum_{F_i\in\mathcal{F}_D}\int_{F_i}\left(n_{i,t}\nabla_x u\cdot\nabla_x v_h-\mathbf{n}_{i,x}\cdot\nabla_x u\partial_t v_h\right)ds.
$$

The jumps of the derivatives of the solution u are zero, i.e., $[\![\nabla_x u]\!]_x=0$ and $[\![\nabla_x u]\!]_t=0$ yielding

$$
=\sum_{i=1}^{N}\int_{Q_i}\left(\nabla_x u\cdot\nabla_x v_h-\theta_i h_i\partial_t\nabla_x u\cdot\nabla_x v_h\right)dxdt+\theta_i h_i\sum_{F_i\in\mathcal{F}_T}\int_{F_i}\nabla_x u\cdot\nabla_x v_h\,ds
$$

$$
+\theta_i h_i\sum_{F_{ij}\in\mathcal{F}_I}\int_{F_{ij}}\{\nabla_x u\}^{up}[\![\nabla_x v_h]\!]_t\,ds-\sum_{F_{ij}\in\mathcal{F}_I}\int_{F_{ij}}\{\nabla_x u\}[\![v_h]\!]_x\,ds
$$

$$
-\theta_i h_i\sum_{F_{ij}\in\mathcal{F}_I}\int_{F_{ij}}\{\nabla_x u\}[\![\partial_t v_h]\!]_x\,ds+\theta_i h_i\sum_{F_i\in\mathcal{F}_D}\int_{F_i}\left(n_{i,t}\nabla_x u\cdot\nabla_x v_h-\mathbf{n}_{i,x}\cdot\nabla_x u\partial_t v_h\right)ds.
$$

Also, for the exact solution u, we have $[\![u]\!]_x=0$ and $[\![\partial_t u]\!]_x=0$ on the interior facets $F_{ij}\in\mathcal{F}_I$. Therefore, we add the following consistent terms:

$$
\sum_{F_{ij}\in\mathcal{F}_I}\int_{F_{ij}}\{\nabla_x v_h\}[\![u]\!]_x\,ds+\theta_i h_i\sum_{F_{ij}\in\mathcal{F}_I}\int_{F_{ij}}\{\nabla_x v_h\}[\![\partial_t u]\!]_x\,ds.
$$

Furthermore, we penalize the interior facets by adding consistency terms that are zero to the bilinear form

$$\sum_{F_{ij} \in \mathcal{F}_I} \int_{F_{ij}} \frac{\delta_1}{h_i} [\![u]\!]_x [\![v_h]\!]_x \, ds + \sum_{F_{ij} \in \mathcal{F}_I} \int_{F_{ij}} \delta_2 \theta_i h_i [\![\partial_t u]\!]_x [\![\partial_t v_h]\!]_x \, ds,$$

where the penalty parameters δ_1 and δ_2 are positive constants that will be determined later. Considering the terms on the Dirichlet facets

$$\sum_{F_i \in \mathcal{F}_D} \int_{F_i} (n_{i,t} \nabla_x u \cdot \nabla_x v_h - \mathbf{n}_{i,x} \cdot \nabla_x u \partial_t v_h) \, ds$$

(3.15)
$$= \sum_{F_i \in \mathcal{F}_D} \int_{F_i} \nabla_x u \cdot (n_{i,t} \nabla_x v_h - \mathbf{n}_{i,x} \partial_t v_h) \, ds.$$

Since $(n_{i,t} \nabla_x v_h - \mathbf{n}_{i,x} \partial_t v_h)$ is the tangential derivative of v_h and $v_h = 0$ on the facets $F_i \in \mathcal{F}_D$, we can proceed as follows:

$$= \sum_{i=1}^N \int_{Q_i} \left(\nabla_x u \cdot \nabla_x v_h - \theta_i h_i \partial_t \nabla_x u \cdot \nabla_x v_h \right) dx dt + \theta_i h_i \sum_{F_i \in \mathcal{F}_T} \int_{F_i} \nabla_x u \cdot \nabla_x v_h \, ds$$

$$+ \theta_i h_i \sum_{F_{ij} \in \mathcal{F}_I} \int_{F_{ij}} \{\nabla_x u\}^{up} [\![\nabla_x v_h]\!]_t \, ds + \sum_{F_{ij} \in \mathcal{F}_I} \int_{F_{ij}} \left(- \{\nabla_x u\} [\![v_h]\!]_x + \{\nabla_x v_h\} [\![u]\!]_x \right) ds$$

$$+ \theta_i h_i \sum_{F_{ij} \in \mathcal{F}_I} \int_{F_{ij}} \left(- \{\nabla_x u\} [\![\partial_t v_h]\!]_x + \{\nabla_x v_h\} [\![\partial_t u]\!]_x \right) ds$$

$$+ \sum_{F_{ij} \in \mathcal{F}_I} \int_{F_{ij}} \left(\frac{\delta_1}{h_i} [\![u]\!]_x [\![v_h]\!]_x + \delta_2 \theta_i h_i [\![\partial_t u]\!]_x [\![\partial_t v_h]\!]_x \right) ds.$$

Next, considering the time derivative term $\partial_t u$, we apply an integration by parts in time as follows:

(3.16)
$$\sum_{i=1}^N \int_{Q_i} \partial_t u v_h \, dx dt = - \sum_{i=1}^N \int_{Q_i} u \partial_t v_h \, dx dt + \sum_{i=1}^N \int_{\partial Q_i} n_{i,t} u v_h \, ds.$$

Rewriting the sum over the boundary integral terms in (3.16), we obtain the following identity:

(3.17)
$$\sum_{i=1}^N \int_{\partial Q_i} n_{i,t} u v_h \, ds = \sum_{F_{ij} \in \mathcal{F}_I} \int_{F_{ij}} [\![u v_h]\!]_t \, ds + \sum_{F_i \in \mathcal{F}_0 \cup \mathcal{F}_T \cup \mathcal{F}_D} \int_{F_i} n_{i,t} u v_h \, ds.$$

Using (3.7) of Lemma 3.2 and the fact that $v_h = 0$ on the facets $F_i \in \mathcal{F}_D \cup \mathcal{F}_0$ and $n_{i,t} = 1$ on $F_i \in \mathcal{F}_T$, the boundary integral term yields

$$\sum_{i=1}^N \int_{\partial Q_i} n_{i,t} u v_h \, ds = \sum_{F_{ij} \in \mathcal{F}_I} \int_{F_{ij}} \left(\{u\}^{up} [\![v_h]\!]_t + \{v_h\}^{down} [\![u]\!]_t \right) ds$$

(3.18)
$$+ \sum_{F_i \in \mathcal{F}_T} \int_{F_i} u v_h \, ds.$$

The jump of u in time direction is zero, i.e., $[\![u]\!]_t = 0$. Thus, we obtain

$$(3.19) \qquad \sum_{i=1}^{N} \int_{\partial Q_i} n_{i,t} u v_h \, ds = \sum_{F_{ij} \in \mathcal{F}_I} \int_{F_{ij}} \{u\}^{up} [\![v_h]\!]_t \, ds + \sum_{F_i \in \mathcal{F}_T} \int_{F_i} u v_h \, ds.$$

In summary, we have shown that the solution u of our strong problem (2.1) fulfills the space-time dGIGA variational identity

$$(3.20) \qquad a_h(u, v_h) = \ell_h(v_h) \quad \forall v_h \in V_{0h},$$

where the bilinear form is represented by

$$a_h(u, v_h) = \sum_{i=1}^{N} \int_{Q_i} \left(-u \partial_t v_h + \theta_i h_i \partial_t u \partial_t v_h + \nabla_x u \cdot \nabla_x v_h - \theta_i h_i \partial_t \nabla_x u \cdot \nabla_x v_h \right) dx dt$$

$$+ \sum_{F_{ij} \in \mathcal{F}_I} \int_{F_{ij}} \{u\}^{up} [\![v_h]\!]_t \, ds + \sum_{F_i \in \mathcal{F}_T} \int_{F_i} u v_h \, ds + \theta_i h_i \sum_{F_i \in \mathcal{F}_T} \int_{F_i} \nabla_x u \cdot \nabla_x v_h \, ds$$

$$+ \theta_i h_i \sum_{F_{ij} \in \mathcal{F}_I} \int_{F_{ij}} \{\nabla_x u\}^{up} [\![\nabla_x v_h]\!]_t \, ds$$

$$+ \sum_{F_{ij} \in \mathcal{F}_I} \int_{F_{ij}} \left(-\{\nabla_x u\} [\![v_h]\!]_x + \{\nabla_x v_h\} [\![u]\!]_x \right) ds$$

$$+ \theta_i h_i \sum_{F_{ij} \in \mathcal{F}_I} \int_{F_{ij}} \left(-\{\nabla_x u\} [\![\partial_t v_h]\!]_x + \{\nabla_x v_h\} [\![\partial_t u]\!]_x \right) ds$$

$$(3.21) \qquad + \sum_{F_{ij} \in \mathcal{F}_I} \int_{F_{ij}} \left(\frac{\delta_1}{h_i} [\![u]\!]_x [\![v_h]\!]_x + \delta_2 \theta_i h_i [\![\partial_t u]\!]_x [\![\partial_t v_h]\!]_x \right) ds$$

and the linear form by

$$(3.22) \qquad \ell(v) = \sum_{i=1}^{N} \int_{Q_i} f \left(v_h + \theta_i h_i \partial_t v_h \right) dx dt.$$

Remark 3.3. We note that the penalty parameters δ_1 and δ_2 in dGIGA are known to depend on the NURBS degree p and dimension of the computational domain d, i.e., $\delta_i = \delta(p, d), i = 1, 2$. The space-time dGIGA is a nonsymmetric discretization scheme.

Next, we show that the bilinear form (3.21) is coercive with respect to the discrete norm

$$\|v_h\|_h^2 = \sum_{i=1}^{N} \|\nabla_x v_h\|_{L_2(Q_i)}^2 + \theta_i h_i \|\partial_t v_h\|_{L_2(Q_i)}^2 + \frac{1}{2} \sum_{F_i \in \mathcal{F}_T} \|v_h\|_{L_2(F_i)}^2$$

$$+ \frac{\theta_i h_i}{2} \sum_{F_i \in \mathcal{F}_T} \|\nabla_x v_h\|_{L_2(F_i)}^2 + \frac{1}{2} \sum_{F_{ij} \in \mathcal{F}_I} \|[\![v_h]\!]_t\|_{L_2(F_{ij})}^2$$

$$+ \frac{\theta_i h_i}{2} \sum_{F_{ij} \in \mathcal{F}_I} \|[\![\nabla_x v_h]\!]_t\|_{L_2(F_{ij})}^2$$

$$(3.23) \qquad + \sum_{F_{ij} \in \mathcal{F}_I} \left(\frac{\delta_1}{h_i} \|[\![v_h]\!]_x\|_{L_2(F_{ij})}^2 + \delta_2 \theta_i h_i \|[\![\partial_t v_h]\!]_x\|_{L_2(F_{ij})}^2 \right).$$

Remark 3.4. The space-time dG norm $\|\cdot\|_h$ from (3.23) is a norm on V_{0h}. Indeed, if $\|v_h\|_h = 0$ for some function $v_h \in V_{0h}$, then $\nabla_x v_h = 0$ and $\partial_t v_h = 0$ in each subdomain Q_i. This means that the function v_h is a constant on each patch Q_i, $i = 1, \ldots, N$. Furthermore, $\|v_h\|_h = 0$ yields that the jumps $[\![v_h]\!]_x, [\![v_h]\!]_t, [\![\partial_t v_h]\!]_x$ and $[\![\nabla_x v_h]\!]_t$ of v_h across the internal facets $F_{ij} \in \mathcal{F}_I$ are zero, i.e., v_h is constant in $\overline{Q}$. Finally, $v_h \in V_{0h}$ implies that v_h is zero on the facets $F_i \in \mathcal{F}_D$ and $F_i \in \mathcal{F}_0$, i.e., this constant must be zero. Therefore, $v_h = 0$ in the whole space-time computational domain Q. The other norm axioms (homogeneity and triangle inequality) are easily verified.

The following lemmata are required to prove the coercivity of the bilinear form.

LEMMA 3.5. *Let $F_{ij} \in \mathcal{F}_I$ be an interior facet and $v \in V_{0h}$ be a function. Then the following identity holds:*

$$\{v\}^{up}[\![v]\!]_t - \frac{1}{2}[\![v^2]\!]_t = \frac{1}{2}|n_{i,t}|[\![v]\!]^2. \tag{3.24}$$

Proof. See, e.g., [24, Lemma 5.19]. □

LEMMA 3.6. *Let K be an arbitrary mesh element from $\mathcal{K}_{h,i}$; the underlying mesh of $Q_i, i = 1, \ldots, N$. Then the inverse inequalities*

$$\|\nabla v\|_{L_2(Q_i)}^2 \leq C_{inv,1,u} h_i^{-2} \|v\|_{L_2(Q_i)}^2 \tag{3.25}$$

and

$$\|v\|_{L_2(\partial Q_i)}^2 \leq C_{inv,0,u} h_i^{-1} \|v\|_{L_2(Q_i)}^2 \tag{3.26}$$

hold for all $v \in V_h$, where $C_{inv,0,u}$ and $C_{inv,1,u}$ are positive constants, which are independent of h_i and Q_i.

Proof. See, e.g., [24, Chapter 2]. □

LEMMA 3.7. *Let $\theta_i > 0$ be sufficiently small such that $\theta_i \leq (C_{inv,0,u} C_q)^{-1}$, where $C_{inv,0,u}$ is chosen as in Lemma 3.6 and C_q satisfies (2.8). Let δ_1 and δ_2 be some positive constants; then the discrete bilinear form $a_h(\cdot, \cdot) : V_{0h} \times V_{0h} \to \mathbb{R}$, defined by (3.21), is V_{0h}-coercive with respect to the norm $\|\cdot\|_h$, i.e.,*

$$a_h(v_h, v_h) \geq \mu_c \|v_h\|_h^2 \quad \forall v_h \in V_{0h}, \tag{3.27}$$

where $\mu_c = 1/2$.

Proof. By using the definition of the bilinear form (3.21), we proceed as follows:

$$\begin{aligned}
a_h(v_h, v_h) = \sum_{i=1}^{N} &-\frac{1}{2} \int_{Q_i} \partial_t v_h^2 \, dxdt + \theta_i h_i \|\partial_t v_h\|_{L_2(Q_i)}^2 + \|\nabla_x v_h\|_{L_2(Q_i)}^2 \\
&- \frac{\theta_i h_i}{2} \int_{Q_i} \partial_t |\nabla_x v_h|^2 \, dxdt + \sum_{F_{ij} \in \mathcal{F}_I} \int_{F_{ij}} \{v_h\}^{up}[\![v_h]\!]_t \, ds + \sum_{F_i \in \mathcal{F}_T} \int_{F_i} v_h^2 \, ds \\
&+ \theta_i h_i \sum_{F_i \in \mathcal{F}_T} \|\nabla_x v_h\|_{L_2(F_i)}^2 + \theta_i h_i \sum_{F_{ij} \in \mathcal{F}_I} \int_{F_{ij}} \{\nabla_x v_h\}^{up}[\![\nabla_x v_h]\!]_t \, ds \\
&+ \sum_{F_{ij} \in \mathcal{F}_I} \left(\frac{\delta_1}{h} \|[\![v_h]\!]_x\|_{L_2(F_{ij})}^2 + \delta_2 \theta_i h_i \|[\![\partial_t v_h]\!]_x\|_{L_2(F_{ij})}^2 \right)
\end{aligned}$$

$$= \sum_{i=1}^{N} \Big(-\frac{1}{2} \int_{\partial Q_i} n_{i,t} v_h^2 \, ds + \theta_i h_i \|\partial_t v_h\|_{L_2(Q_i)}^2 + \|\nabla_x v_h\|_{L_2(Q_i)}^2$$

$$-\frac{\theta_i h_i}{2} \int_{\partial Q_i} n_{i,t} |\nabla_x v_h|^2 \, ds \Big)$$

$$+ \sum_{F_{ij} \in \mathcal{F}_I} \int_{F_{ij}} \{v_h\}^{up} [\![v_h]\!]_t \, ds + \sum_{F_i \in \mathcal{F}_T} \int_{F_i} v_h^2 \, ds$$

$$+ \theta_i h_i \sum_{F_i \in \mathcal{F}_T} \|\nabla_x v_h\|_{L_2(F_i)}^2 + \theta_i h_i \sum_{F_{ij} \in \mathcal{F}_I} \int_{F_{ij}} \{\nabla_x v_h\}^{up} [\![\nabla_x v_h]\!]_t \, ds$$

$$+ \sum_{F_{ij} \in \mathcal{F}_I} \left(\frac{\delta_1}{h} \|[\![v_h]\!]_x\|_{L_2(F_{ij})}^2 + \delta_2 \theta_i h_i \|[\![\partial_t v_h]\!]_x\|_{L_2(F_{ij})}^2 \right).$$

Using Gauss's theorem with $v_h = 0$ on the facet $F_i \in \mathcal{F}_0$, we proceed as follows:

$$= \sum_{i=1}^{N} \Big(\theta_i h_i \|\partial_t v_h\|_{L_2(Q_i)}^2 + \|\nabla_x v_h\|_{L_2(Q_i)}^2 \Big) - \frac{1}{2} \sum_{F_i \in \mathcal{F}_T} \int_{F_i} v_h^2 \, ds - \frac{1}{2} \sum_{F_{ij} \in \mathcal{F}_I} \int_{F_{ij}} [\![v_h^2]\!]_t \, ds$$

$$+ \sum_{F_{ij} \in \mathcal{F}_I} \int_{F_{ij}} \{v_h\}^{up} [\![v_h]\!]_t \, ds + \sum_{F_i \in \mathcal{F}_T} \int_{F_i} v_h^2 \, ds - \frac{\theta_i h_i}{2} \sum_{F_{ij} \in \mathcal{F}_I} \int_{F_{ij}} [\![|\nabla_x v_h|^2]\!]_t \, ds$$

$$- \frac{\theta_i h_i}{2} \sum_{F_i \in \mathcal{F}_T} \|\nabla_x v_h\|_{L_2(F_i)}^2 - \frac{\theta_i h_i}{2} \sum_{F_i \in \mathcal{F}_D} \int_{F_i} n_{i,t} |\nabla_x v_h|^2 \, ds$$

$$+ \theta_i h_i \sum_{F_i \in \mathcal{F}_T} \|\nabla_x v_h\|_{L_2(F_i)}^2 + \theta_i h_i \sum_{F_{ij} \in \mathcal{F}_I} \int_{F_{ij}} \{\nabla_x v_h\}^{up} [\![\nabla_x v_h]\!]_t \, ds$$

$$+ \sum_{F_{ij} \in \mathcal{F}_I} \left(\frac{\delta_1}{h_i} \|[\![v_h]\!]_x\|_{L_2(F_{ij})}^2 + \delta_2 \theta_i h_i \|[\![\partial_t v_h]\!]_x\|_{L_2(F_{ij})}^2 \right)$$

$$= \sum_{i=1}^{N} \Big(\theta_i h_i \|\partial_t v_h\|_{L_2(Q_i)}^2 + \|\nabla_x v_h\|_{L_2(Q_i)}^2 \Big) + \frac{1}{2} \sum_{F_i \in \mathcal{F}_T} \|v_h\|_{L_2(F_i)}^2$$

$$+ \frac{\theta_i h_i}{2} \sum_{F_i \in \mathcal{F}_T} \|\nabla_x v_h\|_{L_2(F_i)}^2 + \sum_{F_{ij} \in \mathcal{F}_I} \int_{F_{ij}} \left(\{v_h\}^{up} [\![v_h]\!]_t - \frac{1}{2} [\![v_h^2]\!]_t \right) ds$$

$$- \frac{\theta_i h_i}{2} \sum_{F_i \in \mathcal{F}_D} \int_{F_i} n_{i,t} |\nabla_x v_h|^2 \, ds + \theta_i h_i \sum_{F_{ij} \in \mathcal{F}_I} \int_{F_{ij}} \left(\{\nabla_x v_h\}^{up} [\![\nabla_x v_h]\!]_t - \frac{1}{2} [\![|\nabla_x v_h|^2]\!]_t \right) ds$$

$$+ \sum_{F_{ij} \in \mathcal{F}_I} \frac{\delta_1}{h_i} \|[\![v_h]\!]_x\|_{L_2(F_{ij})}^2 + \sum_{F_{ij} \in \mathcal{F}_I} \delta_2 \theta_i h_i \|[\![\partial_t v_h]\!]_x\|_{L_2(F_{ij})}^2.$$

Now, by using Lemma 3.5 together with $|n_{i,t}| \geq |n_{i,t}|^2$, we sum over Q_i as follows:

$$= \sum_{i=1}^{N} \Big(\theta_i h_i \|\partial_t v_h\|_{L_2(Q_i)}^2 + \|\nabla_x v_h\|_{L_2(Q_i)}^2 \Big) + \frac{1}{2} \sum_{F_i \in \mathcal{F}_T} \|v_h\|_{L_2(F_i)}^2$$

$$+ \frac{\theta_i h_i}{2} \sum_{F_i \in \mathcal{F}_T} \|\nabla_x v_h\|_{L_2(F_i)}^2 + \frac{1}{2} \sum_{F_{ij} \in \mathcal{F}_I} \int_{F_{ij}} |n_{i,t}| \Big([\![v_h]\!] \Big)^2 ds$$

$$+ \frac{\theta_i h_i}{2} \sum_{F_{ij} \in \mathcal{F}_I} \int_{F_{ij}} |n_{i,t}| \left([\![\nabla_x v_h]\!] \right)^2 ds - \frac{\theta_i h_i}{2} \sum_{F_i \in \mathcal{F}_D} \int_{F_i} n_{i,t} |\nabla_x v_h|^2 ds$$

$$+ \sum_{F_{ij} \in \mathcal{F}_I} \left(\frac{\delta_1}{h} \|[\![v_h]\!]_x\|^2_{L_2(F_{ij})} + \delta_2 \theta_i h_i \|[\![\partial_t v_h]\!]_x\|^2_{L_2(F_{ij})} \right)$$

$$\geq \sum_{i=1}^N \left(\theta_i h_i \|\partial_t v_h\|^2_{L_2(Q_i)} + \|\nabla_x v_h\|^2_{L_2(Q_i)} \right) + \frac{1}{2} \sum_{F_i \in \mathcal{F}_T} \|v_h\|^2_{L_2(F_i)}$$

$$+ \frac{\theta_i h_i}{2} \sum_{F_i \in \mathcal{F}_T} \|\nabla_x v_h\|^2_{L_2(F_i)} + \frac{1}{2} \sum_{F_{ij} \in \mathcal{F}_I} \|[\![v_h]\!]_t\|^2_{L_2(F_{ij})}$$

$$+ \frac{\theta_i h_i}{2} \sum_{F_{ij} \in \mathcal{F}_I} \|[\![\nabla_x v_h]\!]_t\|^2_{L_2(F_{ij})} - \frac{\theta_i h_i}{2} \sum_{F_i \in \mathcal{F}_D} \|\nabla_x v_h\|^2_{L_2(F_i)}$$

$$+ \sum_{F_{ij} \in \mathcal{F}_I} \left(\frac{\delta_1}{h} \|[\![v_h]\!]_x\|^2_{L_2(F_{ij})} + \sum_{F_{ij} \in \mathcal{F}_I} \delta_2 \theta_i h_i \|[\![\partial_t v_h]\!]_x\|^2_{L_2(F_{ij})} \right)$$

$$= \|v_h\|^2_h - \frac{\theta_i h_i}{2} \sum_{F_i \in \mathcal{F}_D} \|\nabla_x v_h\|^2_{L_2(F_i)}.$$

Next, we estimate the term on the facet $F_i \in \mathcal{F}_D$ by using the quasi-uniformity property (2.8) and the inverse inequality (3.26) to arrive at

$$(3.28) \qquad (\theta_i h_i)/2 \sum_{F_i \in \mathcal{F}_D} \|\nabla_x v_h\|^2_{L_2(F_i)} \leq (\theta_i C_q C_{inv,0,u})/2 \sum_{i=1}^N \|\nabla_x v_h\|^2_{L_2(Q_i)}.$$

By using estimate (3.28) and choosing the parameter $\theta_i \leq (C_q C_{inv,0,u})^{-1}$, we obtain

$$a_h(v_h, v_h) \geq \|v_h\|^2_h - (\theta_i C_{inv,0,u} C_q)/2 \sum_{i=1}^N \|\nabla_x v_h\|^2_{L_2(Q_i)}$$

$$\geq (1 - (\theta_i C_{inv,0,u} C_q)/2) \|v_h\|^2_h \geq \frac{1}{2} \|v_h\|^2_h,$$

which completes the proof.

4. Discretization error analysis. In this section, we present a priori error estimates for the space-time scheme. We present the boundedness of the bilinear form. We will require the following trace inequality.

LEMMA 4.1. *Let $Q_i = \Phi_i(\widehat{Q})$ for $i = 1, \ldots, N$. Then the patchwise scaled trace inequality*

$$(4.1) \qquad \|v\|_{L_2(\partial Q_i)} \leq C_{tr,Q} h_i^{-1/2} \left(\|v\|_{L_2(Q_i)} + h_i |v|_{H^1(Q_i)} \right)$$

holds for all $v \in H^1(Q_i)$, where h_i denotes the maximum mesh size in the physical domain, and $C_{tr,Q}$ is a positive constant that only depends on the shape regularity of the mapping Φ_i.

Next, we show the uniform boundedness of the discrete bilinear form $a_h(\cdot, \cdot)$ on $V_{0h,*} \times V_{0h}$, where the space $V_{0h,*} = H^2(Q) + V_{0h}$ is equipped with the norm

$$\|v\|_{h,*}^2 = \|v\|_h^2 + \sum_{i=1}^N (\theta_i h_i)^{-1}\|v\|_{L_2(Q_i)}^2 + (\theta_i h_i)^2\|\partial_t\nabla_x v\|_{L_2(Q_i)}^2$$

$$(4.2) \qquad + \sum_{F_{ij}\in\mathcal{F}_I}\|\{v\}^{up}\|_{L_2(F_{ij})}^2 + \theta_i h_i\sum_{F_{ij}\in\mathcal{F}_I}\|\{\nabla_x v\}^{up}\|_{L_2(F_{ij})}^2 + \sum_{i=1}^N h_i\|\nabla_x v_i\|_{L_2(\partial Q_i)}^2.$$

In order to prove boundedness of the bilinear form $a_h(\cdot,\cdot)$, we need two auxiliary inequalities presented in the following lemma.

LEMMA 4.2. *For positive parameters δ_1 and δ_2, and for $F_{ij}\in\mathcal{F}_I$, the estimates*

$$\left|\int_{F_{ij}}\{\nabla_x u\}[\![v_h]\!]_x\,ds\right| \le \left(\frac{\delta_1^{-1}h_i}{4}(\|\nabla_x u_i\|_{L_2(F_{ij})}^2 + \|\nabla_x u_j\|_{L_2(F_{ij})}^2)\right)^{\frac12}$$

$$(4.3) \qquad\qquad\qquad \times\left(\frac{\delta_1}{h_i}\|[\![v_h]\!]_x\|_{L_2(F_{ij})}^2\right)^{\frac12},$$

$$\left|\theta_i h_i\int_{F_{ij}}\{\nabla_x u\}[\![\partial_t v_h]\!]_x\,ds\right| \le \left(\frac{\delta_2^{-1}\theta_i h_i}{4}(\|\nabla_x u_i\|_{L_2(F_{ij})}^2 + \|\nabla_x u_j\|_{L_2(F_{ij})}^2)\right)^{\frac12}$$

$$(4.4) \qquad\qquad\qquad \times\left(\delta_2\theta_i h_i\|[\![\partial_t v_h]\!]_x\|_{L_2(F_{ij})}^2\right)^{\frac12}$$

hold for all $u\in V_{0h,*}$ and for all $v_h\in V_{0h}$, where h_i is the maximum mesh size of patch Q_i.

Proof. The proof of (4.3) is obtained by using the Cauchy–Schwarz and triangle inequalities and the proof of (4.4) is obtained by means of the Cauchy–Schwarz inequality. See [24, Lemma 6.12]. □

LEMMA 4.3. *The discrete bilinear form $a_h(\cdot,\cdot)$, defined by (3.21), is uniformly bounded on $V_{0h,*}\times V_{0h}$, i.e., there exists a positive constant μ_b that does not depend on h such that*

$$(4.5) \qquad |a_h(u,v_h)| \le \mu_b\|u\|_{h,*}\|v_h\|_h \quad \forall\,u\in V_{0h,*}, \forall\,v_h\in V_{0h}.$$

Proof. Since most of the terms are bounded by using the Cauchy–Schwarz inequality, we will only show the estimates for the other terms. For the next terms, we proceed by using the Cauchy–Schwarz inequality as follows:

$$(4.6) \qquad \sum_{F_{ij}\in\mathcal{F}_I}\int_{F_{ij}}\{\nabla_x v_h\}[\![u]\!]_x\,ds$$

$$\le \left(\sum_{F_{ij}\in\mathcal{F}_I} h_i\delta_1^{-1}\|\{\nabla_x v_h\}\|_{L_2(F_{ij})}^2\right)^{\frac12}\left(\sum_{F_{ij}\in\mathcal{F}_I} h_i^{-1}\delta_1\|[\![u]\!]_x\|_{L_2(F_{ij})}^2\right)^{\frac12}.$$

Considering the first term in (4.6), we apply the quasi-uniformity property (2.8) together with the inverse inequality (3.26) to obtain

$$(4.7) \qquad \sum_{F_{ij}\in\mathcal{F}_I} h_i\delta_1^{-1}\|\{\nabla_x v_h\}\|_{L_2(F_{ij})}^2 \le \sum_{i=1}^N(\delta_1^{-1}C_q C_{inv,0,u})/2\|\nabla_x v_{h,i}\|_{L_2(Q_i)}^2.$$

Using Cauchy–Schwarz we estimate the next term as follows:

$$\theta_i h_i \sum_{F_{ij} \in \mathcal{F}_I} \int_{F_{ij}} \{\nabla_x v_h\} [\![\partial_t u]\!]_x \, ds$$

$$\leq \left(\sum_{F_{ij} \in \mathcal{F}_I} \delta_2^{-1} \theta_i h_i \| \{\nabla_x v_h\} \|^2_{L_2(F_{ij})} \right)^{\frac{1}{2}} \left(\sum_{F_{ij} \in \mathcal{F}_I} \theta_i h_i \delta_2 \| [\![\partial_t u]\!]_x \|^2_{L_2(F_{ij})} \right)^{\frac{1}{2}}.$$

The first term is estimated similarly to (4.7) as follows:

$$\sum_{F_{ij} \in \mathcal{F}_I} \delta_2^{-1} \theta_i h_i \| \{\nabla_x v_h\} \|^2_{L_2(F_{ij})} \leq \sum_{i=1}^N (\theta_i \delta_2^{-1} C_q C_{inv,0,u})/2 \| \nabla_x v_{h,i} \|^2_{L_2(Q_i)}.$$

Using Lemma 4.2, the next terms are estimated by means of the quasi-uniformity property (2.8) as follows:

$$\sum_{F_{ij} \in \mathcal{F}_I} \int_{F_{ij}} \{\nabla_x u\} [\![v_h]\!]_x \, ds$$

$$\leq \left(\delta_1^{-1}/4 \sum_{i=1}^N C_q h_i \| \nabla_x u_i \|^2_{L_2(\partial Q_i)} \right)^{1/2} \left(\sum_{F_{ij} \in \mathcal{F}_I} \frac{\delta_1}{h_i} \| [\![v_h]\!]_x \|^2_{L_2(F_{ij})} \right)^{1/2},$$

$$\theta_i h_i \sum_{F_{ij} \in \mathcal{F}_I} \int_{F_{ij}} \{\nabla_x u\} [\![\partial_t v_h]\!]_x \, ds$$

$$\leq \left(\delta_2^{-1} \theta_i/4 \sum_{i=1}^N C_q h_i \| \nabla_x u_i \|^2_{L_2(\partial Q_i)} \right)^{1/2} \left(\sum_{F_{ij} \in \mathcal{F}_I} \delta_2 \theta_i h_i \| [\![\partial_t v_h]\!]_x \|^2_{L_2(F_{ij})} \right)^{1/2}.$$

Combining the terms from above and using the Cauchy–Schwarz inequality, we obtain

$$|a_h(u, v_h)| \leq \mu_b \|u\|_{h,*} \|v_h\|_h,$$

where $\mu_b = 2\sqrt{\max\{C_{inv,0,u} C_q (\delta_1^{-1} + \theta_i \delta_2^{-1})/4 + 1, (\delta_1^{-1} + \theta_i \delta_2^{-1})/8\}}$.

We recall the local interpolation error estimate as presented in [5], then, using a patchwise interpolation error estimate, we provide an interpolation error estimate in the energy norm. For patch $Q_i, i = 1, \ldots, N$, let $\Pi_{h,i} : L_2(Q_i) \to \mathbb{V}_{h,i}$ denote a quasi interpolant that yields optimal approximation results. We denote Π_h as a combination of $\Pi_{h,1}, \ldots, \Pi_{h,N}$.

PROPOSITION 4.4. *Given the integers l_i and s_i such that $0 \leq l_i \leq s_i \leq p_i + 1$, for a function $v \in H^{s_i}(Q_i)$, then*

$$(4.8) \qquad \sum_{K \in \mathcal{K}_{h,i}} |v - \Pi_{h,i} v|_{H^{l_i}(K)} \leq C_s h_i^{s_i - l_i} \|v\|_{H^{s_i}(Q_i)},$$

where h_i denotes the maximum mesh-size parameter in the physical domain and the constant C_s only depends on l_i, s_i, and p_i, the shape regularity of the physical domain Q_i described by the mapping Φ_i, and, in particular, $\nabla \Phi_i$.

Proof. See, e.g., [30, Proposition 3.1]. □

If the multiplicity of the inner knots is not larger than $p_i + 1 - l_i$, then $\Pi_{h,i}v \in \mathbb{V}_{h,i} \cap H^{l_i}(Q_i), i = 1, \ldots, N$, and estimate (4.8) yields a global estimate.

PROPOSITION 4.5. *Let us assume that the multiplicity of the inner knots is not larger than $p_i + 1 - l_i$. Given the integers l and s such that $0 \leq l_i \leq s_i \leq p_i + 1$, there exist a positive constant C_s such that for a function $v \in H^{s_i}(Q_i)$*

$$(4.9) \qquad |v - \Pi_{h,i}v|_{H^{l_i}(Q_i)} \leq C_s h_i^{(s_i - l_i)} \|v\|_{H^{s_i}(Q_i)},$$

where h_i denotes the maximum mesh-size parameter in the physical domain and the generic constant C_s only depends on $l_i, s_i,$ and p_i, the shape regularity of the physical domain Q_i described by the mapping Φ_i, and, in particular, $\nabla\Phi_i$.

Proof. See, e.g., [30, Proposition 3.2]. $\qquad\qquad\qquad\qquad\qquad\qquad\qquad\qquad\square$

LEMMA 4.6. *Let $\mathbf{s} := \{s_1, \ldots, s_N\}$ contain only integer values, $\mathbf{s} \geq 2$ componentwise, and $v \in H^{\mathbf{s}}(Q, \mathcal{T}_h)$. Then, there exists a projective operator Π_h which is a combination of $\Pi_{h,1}, \ldots, \Pi_{h,N}$ such that $\Pi_{h,i}v \in V_{0h}$ and generic positive constants $C_0, C_1, C_2, C_3, C_4,$ and C_5 such that*

$$(4.10) \qquad \|\nabla(v - \Pi_{h,i}v)\|_{L_2(\partial Q_i)}^2 \leq C_0 h_i^{2(r_i - 1) - 1} \|v\|_{H^{r_i}(Q_i)}^2,$$

$$(4.11) \qquad \sum_{F_{ij} \in \mathcal{F}_I} h \|[\![\nabla_x(v - \Pi_h v)]\!]_t\|_{L_2(F_{ij})}^2 \leq C_1 \sum_{i=1}^N h_i^{2(r_i - 1)} \|v\|_{H^{r_i}(Q_i)}^2,$$

$$(4.12) \qquad \sum_{F_{ij} \in \mathcal{F}_I} \delta_2 \theta_i h_i \|[\![\partial_t(v - \Pi_h v)]\!]_x\|_{L_2(F_{ij})}^2 \leq C_2 \sum_{i=1}^N h_i^{2(r_i - 1)} \|v\|_{H^{r_i}(Q_i)}^2,$$

$$(4.13) \qquad \sum_{F_{ij} \in \mathcal{F}_I} \frac{\delta_1}{h} \|[\![v - \Pi_h v]\!]_x\|_{L_2(F_{ij})}^2 \leq C_3 \sum_{i=1}^N h_i^{2(r_i - 1)} \|v\|_{H^{r_i}(Q_i)}^2,$$

$$(4.14) \qquad \sum_{F_{ij} \in \mathcal{F}_I} \|\{v - \Pi_h v\}^{up}\|_{L_2(F_{ij})}^2 \leq C_4 \sum_{i=1}^N h_i^{2r_i - 1} \|v\|_{H^{r_i}(Q_i)}^2,$$

$$(4.15) \qquad \sum_{F_{ij} \in \mathcal{F}_I} \theta_i h_i \|\{\nabla_x(v - \Pi_h v)\}^{up}\|_{L_2(F_{ij})}^2 \leq C_5 \sum_{i=1}^N h_i^{2(r_i - 1)} \|v\|_{H^{r_i}(Q_i)}^2,$$

where $r_i = \min\{s_i, p_i + 1\}$, and h_i is the mesh size of the patch Q_i in the physical domain, p_i is polynomial degree of the NURBS, δ_1 and δ_2 are positive constants, and the generic constants are independent of the mesh size.

Proof. By using the trace inequality of Lemma 4.1 and the approximation estimate of Proposition 4.5, we proceed with the proof of (4.10) as follows:

$$\|\nabla(v - \Pi_{h,i}v)\|_{L_2(\partial Q_i)}^2$$
$$\leq 2C_{tr,Q}^2 h_i^{-1} \left(\|\nabla(v - \Pi_{h,i}v)\|_{L_2(Q_i)}^2 + h_i^2 |\nabla(v - \Pi_{h,i}v)|_{H^1(Q_i)}^2 \right)$$
$$\leq 2C_s^2 C_{tr,Q}^2 h_i^{-1} \left(h_i^{2(r_i - 1)} \|v\|_{H^{r_i}(Q_i)}^2 + h_i^2 h_i^{2(r_i - 2)} \|v\|_{H^{r_i}(Q_i)}^2 \right)$$
$$\leq C_0 h_i^{2(r_i - 1) - 1} \|v\|_{H^{r_i}(Q_i)}^2, \quad C_0 = 4C_s^2 C_{tr,Q}^2.$$

Since $\nabla = (\nabla_x, \partial_t)^\top$, the approximation (4.10) also holds for both components of the derivative. We will particularly need the following:

$$\|\nabla_x(v - \Pi_{h,i}v)\|_{L_2(\partial Q_i)}^2 \leq C_0 h_i^{2(r_i - 1) - 1} \|v\|_{H^{r_i}(Q_i)}^2,$$

$$(4.16) \qquad \|\partial_t(v - \Pi_{h,i}v)\|^2_{L_2(\partial Q_i)} \leq C_0 h_i^{2(r_i-1)-1} \|v\|^2_{H^{r_i}(Q_i)}.$$

Next, by using Definition 3.1, (4.16), and (4.10) together with (2.8), the proofs of (4.11)–(4.13) are obtained. Since the last two estimates follow the same proof technique, we will show only the proof of (4.15). We estimate the upwind term (4.14). By using Definition 3.1 and (4.10) we proceed as follows:

$$\sum_{F_{ij} \in \mathcal{F}_I} \|\{v - \Pi_h v\}^{up}\|^2_{L_2(F_{ij})}$$

$$\leq 2 \sum_{i=1}^N C_{tr,Q}^2 h_i^{-1} \left(\|v - \Pi_{h,i}v\|^2_{L_2(Q_i)} + h_i^2 |v - \Pi_{h,i}v|^2_{H^1(Q_i)} \right)$$

$$\leq 2C_s^2 C_{tr,Q}^2 \sum_{i=1}^N h_i^{-1} \left(h_i^{2r} \|v\|^2_{H^{r_i}(Q_i)} + h_i^2 h_i^{2(r_i-1)} \|v\|^2_{H^{r_i}(Q_i)} \right)$$

$$\leq 4C_s^2 C_{tr,Q}^2 \sum_{i=1}^N h_i^{2r_i-1} \|v\|^2_{H^{r_i}(Q_i)},$$

which completes the proof. □

Next, we obtain estimates of the approximation error with respect to the discrete norms $\|\cdot\|_h$ and $\|\cdot\|_{h,*}$.

LEMMA 4.7. *Let $s_i, i = 1,\ldots,N$, be a positive integer with $s_i \geq 2$ and $v \in H^{s_i}(Q_i), i = 1,\ldots,N$. Then there exist a projection $\Pi_h v \in V_{0h}$ and generic positive constants C_6 and C_7 such that*

$$(4.17) \qquad \|v - \Pi_h v\|^2_h \leq C_6 \sum_{i=1}^N h_i^{2(r_i-1)} \|v\|^2_{H^{r_i}(Q_i)},$$

$$(4.18) \qquad \|v - \Pi_h v\|^2_{h,*} \leq C_7 \sum_{i=1}^N h_i^{2(r_i-1)} \|v\|^2_{H^{r_i}(Q_i)},$$

where $r_i = \min\{s_i, p_i + 1\}$ and h_i is the mesh size of Q_i, p_i is polynomial degree of the NURBS, and the generic constants C_6 and C_7 are independent of the mesh size h_i.

Proof. Using the definition of the norms $\|\cdot\|_h$ and $\|\cdot\|_{h,*}$ together with Lemma 4.6, we are able to obtain the proof of the statement.

Finally, we present the main result for this chapter, namely, the a priori discretization error estimate in the discrete norm $\|\cdot\|_h$.

THEOREM 4.8. *Let u be the exact solution of our model problem (2.2), and let u_h be the solution to the space-time dGIGA scheme (3.20). Then the discretization error estimate*

$$(4.19) \qquad \|u - u_h\|_h \leq C \sum_{i=1}^N h_i^{r_i-1} \|v\|_{H^{r_i}(Q_i)}$$

holds, where $r_i = \min\{s_i, p_i + 1\}$, C is a generic positive constant independent of the mesh size h_i, and p_i denotes the underlying polynomial degree of the NURBS patch Q_i.

Proof. Subtracting the space-time dGIGA scheme

$$a_h(u_h, v_h) = \ell_h(v_h) \quad \forall v_h \in V_{0h}$$

from the consistency identity

$$a_h(u, v_h) = \ell_h(v_h) \quad \forall v_h \in V_{0h},$$

we obtain the so-called Galerkin orthogonality

$$(4.20) \qquad\qquad a_h(u - u_h, v_h) = 0 \quad \forall v_h \in V_{0h},$$

which is crucial for the discretization error estimate. Using now the triangle inequality, we can estimate the discretization error $u - u_h$ as follows:

$$(4.21) \qquad\qquad \|u - u_h\|_h \le \|u - \Pi_h u\|_h + \|\Pi_h u - u_h\|_h.$$

The first term is estimated by Lemma 4.7. The estimation of the second term on the right-hand side of (4.21) follows by using the fact that $\Pi_h u - u_h \in V_{0h}$, the ellipticity of the bilinear form $a_h(\cdot, \cdot)$ as was shown in Lemma 3.7, the Galerkin orthogonality (4.20), and the boundedness of the discrete bilinear form Lemma 4.3, and we can derive the following estimates:

$$\mu_c \|\Pi_h u - u_h\|_h^2 \le a_h(\Pi_h u - u_h, \Pi_h u - u_h) = a_h(\Pi_h u - u, \Pi_h u - u_h)$$
$$\le \mu_b \|\Pi_h u - u\|_{h,*} \|\Pi_h u - u_h\|_h.$$

Hence, we have

$$(4.22) \qquad\qquad \|\Pi_h u - u_h\|_h \le (\mu_b/\mu_c)\|\Pi_h u - u\|_{h,*}.$$

Inserting (4.22) into the triangle inequality (4.21) and using the estimates (4.18) and (4.17) from Lemma 4.7, we have

$$\begin{aligned}
\|u - u_h\|_h &\le \|u - \Pi_h u\|_h + \|\Pi_h u - u_h\|_h \\
&\le \|u - \Pi_h u\|_h + (\mu_b/\mu_c)\|\Pi_h u - u\|_{h,*} \\
&\le (C_6 + (\mu_b/\mu_c)C_7) \sum_{i=1}^N h_i^{r_i - 1} \|u\|_{H^{r_i}(Q_i)},
\end{aligned}$$

which proves the discretization error estimate (4.19) with $C = (C_6 + (\mu_b/\mu_c)C_7)$.

5. Numerical results. The numerical results presented below have been performed in G+SMO; see [15]. We used the sparse direct solver SuperLU to solve the resulting linear system of space-time dGIGA equations. We present numerical results for two- and three-dimensional spatial computational domains with the parameter $\theta_i = 0.1, i = 1, \ldots, N$, in all our numerical experiments in the space-time dG-norm as well as the L_2-norm. We assume in all our experiments that the B-spline degree in both space direction and time direction are equal. We also note that the B-spline degrees on all the patches are equal and denoted by p, i.e., $p = p_i, i = 1, \ldots, N$. The penalty parameters are chosen as $\delta_1 = \delta_2 = 2(p+d+1)(p+1)$. In our numerical experiments on the convergence behavior of the space-time dGIGA methods proposed, we have used B-splines of polynomial degrees $p = 1, 2, 3, 4$ and computed the rate of convergence of successive mesh refinement by means of the formula $\log_2(\|\cdot\|_{h,i+1}/\|\cdot\|_{h,i})$.

5.1. Two-dimensional space-time computational domain. We consider a space-time computational domain $Q = \{(x, t) \in \mathbb{R}^2 : x \in \Omega(t), t \in (0, 2)\}$ with a one-dimensional moving spatial computational domain of the form $\Omega(t) = \{x \in \mathbb{R} : a(t) < x < b(t)\}$, $t \in (0, 2)$, where $a(t) = -t(1-t)/2$ and $b(t) = 1 - t(1-t)/2$ for $t \in [0, 1]$, whereas $a(t) = -(t-1)(t-2)/2$ and $b(t) = (t^2 - 3t + 4)/2$ for $t \in [1, 2]$, leading to the decomposition of the space-time cylinder $\overline{Q} = \overline{Q}_2 \cup \overline{Q}_1$ into the two nonoverlapping

patches $Q_2 = \{(x,t) \in \mathbb{R}^2 : x \in \Omega(t), t \in (0,1)\}$ and $Q_1 = \{(x,t) \in \mathbb{R}^2 : x \in \Omega(t), t \in (1,2)\}$, respectively. The two patches Q_1 and Q_2 can also be represented by knot vectors such that $Q_1 = \{\Xi_1 := \{0,0,1,1\}, \Xi_2 := \{0,0,0,1,1,1\}\}$, and $Q_2 = \{\Xi_1 := \{0,0,1,1\}, \Xi_2 := \{0,0,0,1,1,1\}\}$ with the corresponding control points $\mathbf{P}_{1,1}^1 = (0,1)$, $\mathbf{P}_{2,1}^1 = (1,1)$, $\mathbf{P}_{2,2}^1 = (0.25,1.5)$, $\mathbf{P}_{2,3}^1 = (0.75,1.5)$, $\mathbf{P}_{1,3}^1 = (0,2)$, and $\mathbf{P}_{1,2}^1 = (1,2)$ and $\mathbf{P}_{1,1}^2 = (0,0)$, $\mathbf{P}_{2,1}^2 = (1,0)$, $\mathbf{P}_{2,2}^2 = (-0.25,0.5)$, $\mathbf{P}_{2,3}^2 = (1.25,0.5)$, $\mathbf{P}_{1,3}^2 = (0,1)$, and $\mathbf{P}_{1,2}^2 = (1,1)$, respectively. We again solve our model problem (2.1) and choose the data such that the solution is given by $u(x,t) = \sin(\pi x)\sin(\pi t)$, i.e., $f(x,t) = \partial_t u(x,t) - \Delta u(x,t) = (\pi \sin(\pi x))(\cos(\pi t) + \pi \sin(\pi t))$ in Q, $u_0 = 0$ on $\overline{\Omega}$, and $u(x,t) = \sin(\pi x)\sin(\pi t)$ on Σ. Thus, the compatibility condition between boundary and initial conditions holds. The convergence behavior of the space-time dGIGA scheme with respect to the discrete norm $\|\cdot\|_h$ is presented in Table 1 by a series of h-refinements and by using B-splines of polynomial degrees $p = 2,3,4$ and $p = 5$. After some saturation, we observe the optimal convergence rate $O(h^p)$ for $p \geq 2$ as theoretically predicted by Theorem 4.8 for smooth solutions. Finally, the contour plot of the solution can be seen in Figure 4.

TABLE 1

The degrees of freedom (Dof) and error estimates of the discrete norm $\|\cdot\|_h$ for the computational domain $Q \subset \mathbb{R}^2$ using B-spline degree $p = 2,3,4$ and $p = 5$.

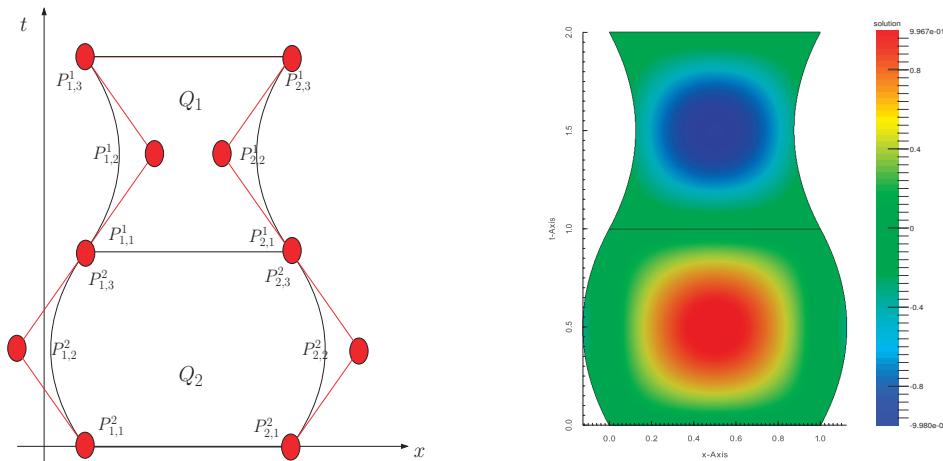| $p = 2$		$p = 3$		$p = 4$		$p = 5$	
Dof	$\|\cdot\|_h$	Dof	$\|\cdot\|_h$	Dof	$\|\cdot\|_h$	Dof	$\|\cdot\|_h$
18	1.503820	32	0.670991000	50	8.44729e-01	7.2000e01	3.5500e-02
32	0.753035	50	0.114153000	72	3.02889e-02	9.8000e01	1.8268e-02
72	0.290070	98	0.022243000	128	2.85575e-03	1.6200e02	4.5179e-04
200	0.139762	242	0.004577210	288	2.86516e-04	3.3800e02	1.2524e-05
648	0.069386	722	0.001095890	800	3.37435e-05	8.8200e02	6.5402e-07
2312	0.034640	2450	0.000270950	2592	4.16219e-06	2.7380e03	4.0153e-08
8712	0.017314	8978	0.000067517	9248	5.18830e-07	9.5220e03	2.5205e-09

FIG. 4. *Multipatch space-time computational domain with control points (left) and solution contours (right) for Example* 5.1.

5.2. Three-dimensional space-time computational domain. We again consider a three-dimensional space-time computational domain $Q = \{(x,t) \in \mathbb{R}^3 : x \in \Omega(t), t \in (0,2)\} \subset \mathbb{R}^3$. The space-time cylinder is decomposed as $\overline{Q} = \overline{Q_2} \cup \overline{Q_1}$ into

TABLE 2

The control points $\mathbf{P}^1_{i_1,i_2,i_3}$ and $\mathbf{P}^2_{i_1,i_2,i_3}$ corresponding to patches Q_1 and Q_2 as depicted in Figure 5.

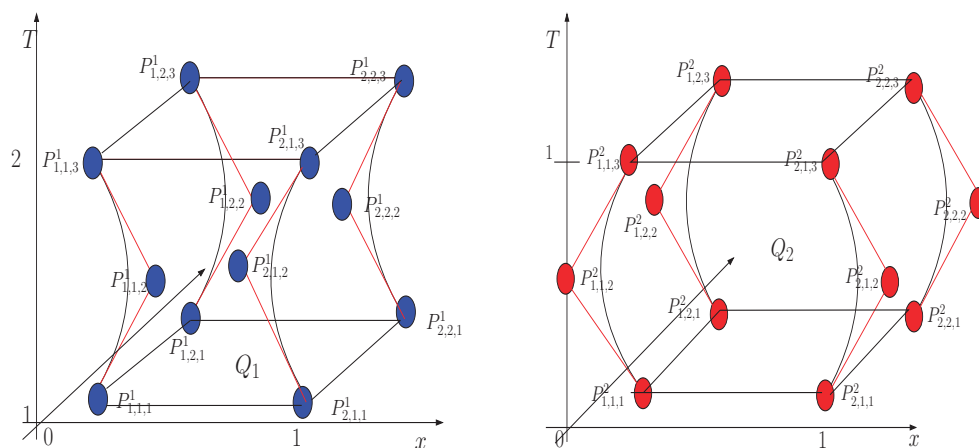| i_1	i_2	i_3	$\mathbf{P}^1_{i_1,i_2,i_3}$	$\mathbf{P}^2_{i_1,i_2,i_3}$
1	1	1	$(0,0,1)$	$(0,0,0)$
1	1	2	$(0.25,0,1.5)$	$(-0.25,0,0.5)$
1	1	3	$(0,0,2)$	$(0,0,1)$
1	2	1	$(0,1,1)$	$(0,1,0)$
1	2	2	$(0.25,1,1.5)$	$(-0.25,1,0.5)$
1	2	3	$(0,1,2)$	$(0,1,1)$
2	1	1	$(1,0,1)$	$(1,0,0)$
2	1	2	$(0.75,0,1.5)$	$(1.25,0,0.5)$
2	1	3	$(1,0,2)$	$(1,0,1)$
2	2	1	$(1,1,1)$	$(1,1,0)$
2	2	2	$(0.75,1,1.5)$	$(1.25,1,0.5)$
2	2	3	$(1,1,2)$	$(1,1,1)$

FIG. 5. *The control points of the decomposed space-time computational domain consisting of patches Q_1 (left) and Q_2 (right).*

the two nonoverlapping patches $Q_2 = \{(x,t) \in \mathbb{R}^3 : x \in \Omega(t)\}, t \in (0,1)$, and $Q_1 = \{(x,t) \in \mathbb{R}^3 : x \in \Omega(t)\}, t \in (1,2)$. The two patches Q_1 and Q_2 can also be represented by knot vectors such that $Q_1 = \{\Xi_1 := \{0,0,1,1\}, \Xi_2 := \{0,0,1,1\}, \Xi_3 := \{0,0,0,1,1,1\}\}$ and $Q_2 = \{\Xi_1 := \{0,0,1,1\}, \Xi_2 := \{0,0,1,1\}, \Xi_3 := \{0,0,0,1,1,1\}\}$ with the corresponding control points $\mathbf{P}^1_{i_1,i_2,i_3}$ and $\mathbf{P}^2_{i_1,i_2,i_3}$, presented in Table 2. We solve our model problem (2.1) and again choose the data such that the solution is given by $u(x,t) = \sin(\pi x)\sin(\pi t)$, i.e., $f(x,t) = \partial_t u(x,t) - \Delta u(x,t) = (\pi \sin(\pi x))(\cos(\pi t) + \pi \sin(\pi t))$ in Q, $u_0 = 0$ on $\overline{\Omega}$, and $u(x,t) = \sin(\pi x)\sin(\pi t)$ on Σ. Thus, the compatibility condition between boundary and initial conditions holds. The convergence behavior of the space-time dGIGA scheme with respect to the space-time dG norm $\|\cdot\|_h$ is shown in Table 3 by a series of h-refinement and by using B-splines of polynomial degrees $p = 2, 3, 4$ and $p = 5$. After some saturation, we observe the optimal convergence rate $O(h^p)$ for $p \geq 2$ as theoretically predicted by Theorem 4.8 for smooth solutions. The plot of the solution can be seen in Figure 6.

6. Conclusion. In this paper, we presented a space-time multipatch discontinuous Galerkin isogeometric analysis, or dGIGA, for parabolic evolution problems.

TABLE 3

The degrees of freedom (Dof) and error estimate of the discrete norm $\|\cdot\|_h$ for the computational domain $Q \subset \mathbb{R}^3$ using B-spline degree $p = 2, 3, 4$ and $p = 5$.

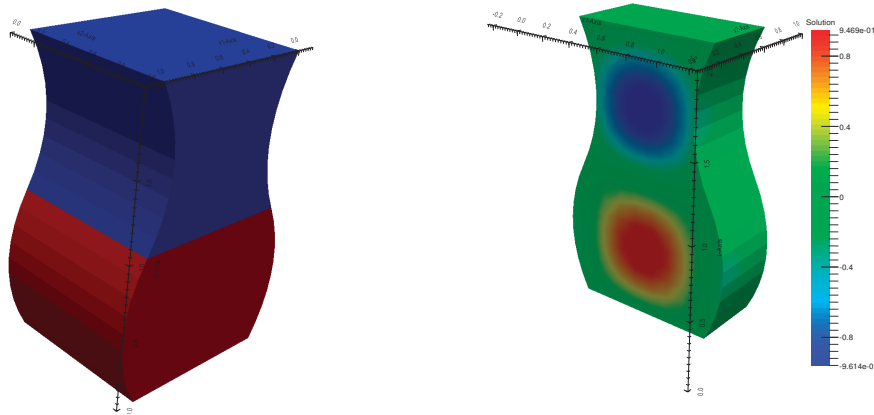| $p = 2$		$p = 3$		$p = 4$		$p = 5$	
Dof	$\|\cdot\|_h$	Dof	$\|\cdot\|_h$	Dof	$\|\cdot\|_h$	Dof	$\|\cdot\|_h$
48	1.690800	116	$5.0517e-01$	230	$6.9387e-00$	300	$3.6137e-02$
116	0.749990	230	$1.6916e-01$	402	$2.8799e-02$	504	$1.5230e-02$
402	0.324060	644	$3.1980e-02$	968	$4.0807e-03$	152	$1.3290e-03$
1910	0.159230	2552	$7.2383e-03$	3324	$4.4778e-04$	3744	$7.2569e-05$
11358	0.079375	13376	$1.7696e-03$	15620	$5.3989e-05$	16800	$4.4531e-06$
77486	0.039663	84560	$4.3993e-04$	92052	$6.6883e-06$	95904	$2.7981e-07$

FIG. 6. *The multipatch space-time computational domain (left) and the solution contours for Example 5.2 (right).*

Parabolic evolution problems are usually solved by a time-stepping scheme. However, by using a time-upwind test function, we derive a stable or elliptic space-time multi-patch scheme. We applied a dG methodology in both space and time and derived a stable space-time dG scheme. We showed optimal a priori error estimates with respect to a space-time dG norm $\|\cdot\|_h$. Finally, we presented convincing numerical experiments for the scheme including two- and three-dimensional computational domains. The current scheme can be combined with surface PDEs as presented in [22]. An extension of the analysis to include low regularity space-time solutions, i.e., $u \in W^{2,q}(Q), q \in (2d/(d+2), 2]$ and $d \in \{2, 3, 4\}$, will be considered in the future.

Acknowledgment. The author would like to thank the reviewers for the valuable information and corrections to this article.

REFERENCES

[1] R. ANDREEV, *Stability of sparse space-time finite element discretizations of linear parabolic evolution equations*, IMA J. Numer. Anal., 33 (2013), pp. 242–260.

[2] I. BABUŠKA AND T. JANIK, *The h-p version of the finite element method for parabolic equations. I. The p-version in time*, Numer. Methods Partial Differential Equations, 5 (1989), pp. 363–399.

[3] I. BABUŠKA AND T. JANIK, *The h-p version of the finite element method for parabolic equations. II. The h-p version in time*, Numer. Methods Partial Differential Equations, 6 (1990), pp. 343–369.

[4] R. E. Bank, P. S. Vassilevski, and L. T. Zikatanov, *Arbitrary dimension convection-diffusion schemes for space-time discretizations*, J. Comput. Appl. Math., 310 (2017), pp. 19–31, https://doi.org/10.1016/j.cam.2016.04.029.

[5] Y. Bazilevs, L. Beirão da Veiga, J. A. Cottrell, T. J. R. Hughes, and G. Sangalli, *Isogeometric analysis: Approximation, stability and error estimates for h-refined meshes*, Comput. Methods Appl. Mech. Engrg., 194 (2006), pp. 4135–4195.

[6] M. Behr, *Simplex space-time meshes in finite element simulations*, Internat. J. Numer. Methods Fluids, 57 (2008), pp. 1421–1434.

[7] E. Brivadis, A. Buffa, B. Wohlmuth, and L. Wunderlich, *Isogeometric mortar methods*, Comput. Methods Appl. Mech. Engrg., 284 (2015), pp. 292–319.

[8] N. Chegini and R. Stevenson, *Adaptive wavelet schemes for parabolic problems: Sparse matrices and numerical results*, SIAM J. Numer. Anal., 49 (2011), pp. 182–212.

[9] J. A. Cottrell, T. J. R. Hughes, and Y. Bazilevs, *Isogeometric Analysis: Toward Integration of CAD and FEA*, John Wiley & Sons, Chichester, UK, 2009.

[10] D. A. Di Pietro and A. Ern, *Mathematical Aspects of Discontinuous Galerkin Methods*, Math. Appl. 69, Springer-Verlag, Berlin, 2012.

[11] P. Hansbo, *Space-time oriented streamline diffusion methods for nonlinear conservation laws in one dimension*, Comm. Numer. Methods Engrg., 10 (1994), pp. 203–215.

[12] T. J. R. Hughes, J. A. Cottrell, and Y. Bazilevs, *Isogeometric analysis: CAD, finite elements, NURBS, exact geometry and mesh refinement*, Comput. Methods Appl. Mech. Engrg., 194 (2005), pp. 4135–4195.

[13] T. J. R. Hughes and G. M. Hulbert, *Space-time finite element methods for elastodynamics: Formulations and error estimates*, Comput. Methods Appl. Mech. Engrg., 66 (1988), pp. 339–363.

[14] C. Johnson, *Numerical Solution of Partial Differential Equations by the Finite Element Method*, Dover, Mineola, NY, 2009.

[15] B. Jüttler, U. Langer, A. Mantzaflaris, S. E. Moore, and W. Zulehner, *Geometry + Simulation Modules: Implementing Isogeometric Analysis*, PAMM, 14 (2014), pp. 961–962.

[16] C. M. Klaij, J. J. W. van der Vegt, and H. van der Ven, *Space-time discontinuous Galerkin method for the compressible Navier-Stokes equations*, J. Comput. Phys., 217 (2006), pp. 589–611, https://doi.org/10.1016/j.jcp.2006.01.018.

[17] P. Knabner and L. Angermann, *Numerical Methods for Elliptic and Parabolic Partial Differential Equations*, Texts in Appl. Math., Springer New York, 2006.

[18] O. A. Ladyzhenskaya, V. A. Solonnikov, and N. N. Uraltseva, *Linear and Quasilinear Equations of Parabolic Type*, Nauka, Moscow, 1967 (in Russian).

[19] O. A. Ladyzhenskaya, V. A. Solonnikov, and N. N. Uraltseva, *Linear and Quasi-Linear Equations of Parabolic Type*, Transl. Math. Monogr. 23, AMS, Providence, RI, 1968.

[20] J. Lang, *Adaptive Multilevel Solution of Nonlinear Parabolic PDE Systems. Theory, Algorithm, and Applications*, vol. 16 of Lecture Notes in Computational Sciences and Engineering, Springer Verlag, Heidelberg, Berlin, 2000.

[21] U. Langer, A. Mantzaflaris, S. E. Moore, and I. Toulopoulos, *Multipatch discontinuous galerkin isogeometric analysis*, in Isogeometric Analysis and Applications 2014, B. Jüttler and B. Simeon, eds., Lect. Notes Comput. Sci. Eng. 107, Springer, New York, 2015, pp. 1–32.

[22] U. Langer and S. E. Moore, *Discontinuous Galerkin isogeometric analysis of elliptic PDEs on surfaces*, in Domain Decomposition Methods in Science and Engineering XXII, T. Dickopf, J. M. Gander, L. Halpern, R. Krause, and F. L. Pavarino, eds., Springer, New York, 2016, pp. 319–326.

[23] U. Langer, S. E. Moore, and M. Neumüller, *Space-time isogeometric analysis of parabolic evolution equations*, Comput. Methods Appl. Mech. Engrg., 306 (2016), pp. 342–363.

[24] S. E. Moore, *Nonstandard Discretization Strategies in Isogeometric Analysis for Partial Differential Equations*, Ph.D. thesis, Johannes Kepler University, Linz, Austria, 2017.

[25] S. E. Moore, *A stable space–time finite element method for parabolic evolution problems*, Calcolo, 55 (2018), 18, https://doi.org/10.1007/s10092-018-0261-8.

[26] M. Neumüller and O. Steinbach, *A DG space–time domain decomposition method*, in Domain Decomposition Methods in Science and Engineering XX, R. Bank, M. Holst, O. Widlund, and J. Xu, eds., Springer, New York, 2013, pp. 623–630.

[27] S. Rhebergen, B. Cockburn, and J. J. W. van der Vegt, *A space-time discontinuous Galerkin method for the incompressible Navier-Stokes equations*, J. Comput. Phys., 233 (2013), pp. 339–358, https://doi.org/10.1016/j.jcp.2012.08.052.

[28] D. Schötzau and C. Schwab, *An hp a priori error analysis of the DG time-stepping method for initial value problems*, Calcolo, 37 (2000), pp. 207–232.

[29] C. Schwab and R. Stevenson, *Space–time adaptive wavelet methods for parabolic evolution problems*, Math. Comp., 78 (2009), pp. 1293–1318.

[30] A. Tagliabue, L. Dede, and A. Quarteroni, *Isogeometric analysis and error estimates for high order partial differential equations in fluid dynamics*, Comput. & Fluids, 102 (2014), pp. 277–303.

[31] T. E. Tezduyar, M. Behr, S. Mittal, and J. Liou, *A new strategy for finite element computations involving moving boundaries and interfaces—the deforming-spatial-domain/space-time procedure. I: The concept and the preliminary numerical tests*, Comput. Methods Appl. Mech. Engrg., 94 (1992), pp. 339–351.

[32] V. Thomée, *Galerkin Finite Element Methods for Parabolic Problems*, Springer Ser. Comput. Math., Springer, New York, 2006.

[33] K. Urban and A. T. Patera, *An improved error bound for reduced basis approximation of linear parabolic problems*, Math. Comp., 83 (2014), pp. 1599–1615.

[34] J. van der Vegt, *Space-time discontinuous Galerkin finite element methods*, VKI Lecture Series, Von Karman Institute for Fluid Dynamics, 2006, pp. 1–37.

[35] J. Wloka, *Partielle Differentialgleichungen*, Teubner Verlag, Stuttgart, 1982.

[36] J. Wloka, *Partial Differential Equations*, Cambridge University Press, Cambridge, UK, 2012.